in : Advances in Surface Treatments (ed. by A. Niku-Lari), Vol. 4 Internat. Guidebook on Residual Stresses Pergamon Press, 1987

RELAXATION OF RESIDUAL STRESSES BY ANNEALING OR MECHANICAL TREATMENT

O. Vöhringer

Institut für Werkstoffkunde I, Universität Karlsruhe (TH), FRG

ABSTRACT

The current knowledge of the relaxation of residual stresses is presented in a condensed and, as far as possible, systematic form. During subjection to thermal or mechanical energy at not too high temperatures the residual stress relaxation is caused by an oriented slip of dislocations which transforms elastic residual strains into microplastic strains. Relaxation will be found as soon as residual stresses - possibly superimposed with external stresses of the same orientation - locally exceed the resistance for onset of plastic deformation. The effect of characteristic properties on the onset and rate of relaxation of residual stresses by annealing, uniaxial and cyclic deformation will be verified by typical examples of experimental results. Possible formulae which can be used to quantify residual stress relaxation are considered and the underlying mechanisms are discussed.

NOMENCLATURE

A^c	area of cross-section in the core region
A^s	area of cross-section in the surface region
E	Young's modulus
k	Boltzmann constant
m	exponent in Avrami equation
N	number of cycles
N_f	number of cyles to failure
Q	activation energy for relaxation of residual stresses
Q_o	activation energy for self diffusion
Q_1	activation energy for diffusion of interstition atoms
R_e	yield point
$\bar{R}_e$	composite yield point
R_e^s	surface yield point
R_e^c	core yield point
$R_{e,c}$	creep resistance
$R_{e,cyc}$	cyclic yield point

R_i	materials resistance
$R_{p0.01}$	0.01% proof stress
$R_{p\varepsilon}$	proof stress at ε_p plastic strain
R_m	tensile strength
ε_e	elastic strain
$\varepsilon_{e,rs}$	elastic residual strain
ε_p	plastic strain
ε_t	total strain
ε_t^*	critical strain (at $\sigma_{rs} = 0$)
σ	normal stress
$\bar{\sigma}$	overall stress
σ^c	core stress
σ^s	surface stress
σ_a	stress amplitude
σ_e	effective stress
σ_{rs}	residual stress
σ^c_{rs}	residual stress in the core
σ^s_{rs}	residual stress at the surface
$\sigma_1;\sigma_2;\sigma_3$	principal stress
$\sigma_{1,rs};\sigma_{2,rs};\sigma_{3,rs}$	principal residual stress
ρ_t	total dislocation density

INTRODUCTION

The residual stresses, formed in components during production or operation, may have considerable practical significance. They take effect on the deformation and failure behaviour of the components under quasistatic or cyclic load. The stability or relaxation behaviour of these residual stresses is thus of fundamental and practical interest. Stable residual stresses are frequently desirable, for example where compressive residual stresses are deliberately set up in the surface regions of structural components in order to improve their fatigue strength. On the other hand there are examples of the deleterious effects of stable residual stresses such as stress relief cracking, stress corrosion, fretting and warping. If residual stresses are relaxed by annealing or mechanical treatment they naturally have little if any influence on subsequent component failure.

Residual stresses can be reduced or completely relaxed by the application of mechanical and/or thermal energy. The elastic residual strains ε_e associated with the residual stresses via Hooke's law can be converted into micro-plastic strains ε_p by suitable deformation processes. This transformation can, for example, be achieved by dislocation slip, dislocation creep, grain boundary sliding and/or diffusion creep. If these processes occur to only a limited extent or not at all, relaxation of residual stresses is also conceivable by crack formation and propagation. Relaxation of residual stresses in the real case occurs by complex interaction of a large number of factors. It depends not only on the residual stress state itself but also on the state, on the condition of the load, on the geometry and the environment of the materials.

The best known and most important techniques which bring about residual stress-relaxation [cf. 1-12] are

annealing (tempering)

uniaxial deformation (drawing, stretching)

cyclic deformation.

Also relaxation of residual stresses can be caused [5,6] by

temperature cyclic loading

quenching

neutron bombardment

the effect of alternating magnetic fields (in the use of ferromagnetics)

vibration

partial damage.

In only very few cases the relaxation behaviour of residual stresses of different technological origin was analysed systematically [cf. 6,7,13-22]. This is understandable on account of the considerable experimental effort it entails. Before the effect of applied thermal or mechanical energy on the residual stress state can be assessed, the latter must be determined quantitatively. In the case of mechanical techniques the necessarily large number of measurements involve considerable expenditure of both time and money. Most investigations have therefore employed X-ray methods.

In the following review, which is a revised and updated version of [12], current knowledge of residual stress-relaxation is presented in a condensed and, as far as possible, systematic form. The abundance of available experimental data nevertheless necessitates a limitation to the scope of this review. Thus the findings of residual stress-relaxation by annealing, uniaxial and cyclic deformation will be taken as examples which demonstrate universally valid rules. Possible formulae which can be used to quantify residual stress-relaxation are discussed and the underlying structure-mechanical mechanisms considered.

RELAXATION OF RESIDUAL STRESSES BY ANNEALING

Thermally Activated Processes

If a material is annealed for several hours at a temperature of

$$T \approx 0.5\ T_m[K] \qquad (1)$$

where T_m is the melting temperature, and then cooled slowly to room temperature, almost total relaxation of the residual stresses arising from forming, machining, heat treatment of joining operations can be achieved. The necessary annealing time depends essentially on the dimensions of the workpiece and of the material state. Since an annealing temperature of $0.5\ T_m$ lies in the region of the recrystallization temperature, complete relaxation of residual macrostresses can be expected. Residual microstresses are considerably reduced but not entirely removed, since lattice defects, in particular dislocations, and in the case of heterogeneous materials the different expansion coefficients of the various phases are always responsible for some residual microstresses. Residual stress-relaxation by annealing is brought about by so-called thermally activated processes

for which the annealing temperature and duration are interchangeable within certain limits. In order to achieve comparable residual stress-relaxation at a lower annealing temperature, the annealing time must be increased correspondingly.

Thermal residual stress-relaxation is fundamentally affected by the residual stress state itself and by the material state. This is convincingly demonstrated by the findings presented in Figs. 1 and 2 [11,19,23], which show the effect of one hour anneals on the residual surface stresses of a variety of origins in a variety of steels measured using X-ray methods. Fig. 1 is a bar chart showing the residual stresses present in the original state and after the normal industrial stress relieving for hardened components of 1 h at 200°C. The materials deformed in tension have undergone negligible residual stress-relaxation. The residual stress-relaxation produced by annealing of surface machined specimens (11% for a plain carbon steel with 0.45 wt.-% carbon, German grade, Ck 45 (c), 17% for Ck 45 (d) and 19% for the rolling bearing steel 100 Cr 6) is greater, the greater the original residual compressive stresses. The most pronounced relative residual stress-relaxation is, however, observed in the hardened materials (25% for Ck 22 - plain carbon steel with 0.22 wt.-% carbon - and 37% for Ck 45). Figure 2 shows the relative residual stresses $\sigma_{rs}(T)/\sigma_{rs}(293K)$ for the same materials as a function of the homologous annealing temperature T/T_m. It can be seen that a one hour anneal at 0.5 T_m (about 600°C) results in every case in complete relaxation of the macrostresses. Characteristic, material-specific stress-temperature curves are obtained. Clearly, residual stress produced by hardening are relaxed at lower temperatures, machining residual stresses at medium temperatures and deformation residual stresses at higher temperatures. In order to achieve the same degree of residual stress-relaxation, for example, 50%, in one hour in hardened and in deformed Ck 45, a temperature difference of 150°C is necessary. Furthermore, according to Fig. 1, larger initial residual stresses result in a shift of the σ_{rs}-T curve to lower annealing temperature in the case of hardened or machined material.

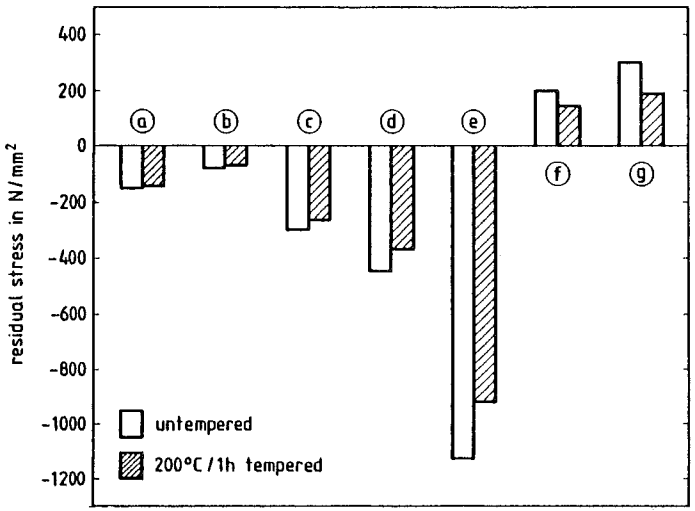

Fig. 1 Residual stresses σ_{rs} of different steels before and after tempering of 1 h at 200°C [11,19,23] (a) Ck 45, normalized and tensile strained (ϵ_p = 5%) (b) Ck 22, normalized and tensile strained (ϵ_p = 5%) (c) Ck 45, normalized and ground, (d) Ck 45, normalized and ground, (e) 100 Cr 6, hardend and shot peened, (f) Ck 22, hardened, (g) Ck 45, hardened.

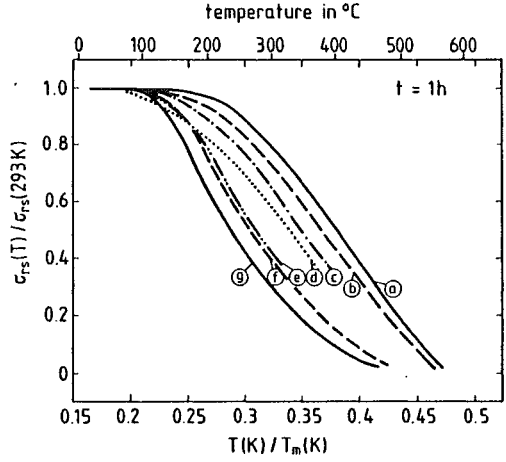

Fig. 2 Influence of homologous temperature T/T_m on residual stress ratio $\sigma_{rs}(T)/\sigma_{rs}(293K)$ of stels, annealed 1 h. (a) to (g) as in Fig. 1.

Residual microstresses and their relaxation behaviour can be determined from the full width at half maximum of the X-ray interference lines using a relationship given in [19]. Again, the residual microstresses in steels are more effectively relaxed at a higher temperature and analogously to the residual macrostresses (cf. Fig. 2) machining residual microstresses are relaxed at lower temperatures as those produced by deformation in tension. In comparable steels, residual microstresses are relaxed after a longer period or at a higher temperature than residual macrostresses [12,19]. In order to achieve 50% residuals microstress-relaxation in tensile-deformed Ck 45, for example, annealed for 1 h, the annealin temperature must be 100°C higher than that needed to achieve the same degree of relaxation from residual macrostresses.

Data of the thermal residual microstress-relaxation for hardened steels are not available. Indications of the relaxation behaviour are however given by the analyses of X-ray interference lines produced by carbon steels in [24]. The mean lattice distortions $\langle\varepsilon^2\rangle^{1/2}$ which are proportional to the residual microstresses, increase with increasing carbon content due to the increasing number of octahedrally dissolved carbon atoms in the body centred tetragonal martensite lattice and also to the increasing dislocation density [25]. The greater the carbon content the lower the temperature for the onset of residual stress-relaxation and the greater the recovery rate. These findings indicate that for hardened materials and with increasing carbon content the relaxation of residual microstresses occurs more rapidly and at lower temperatures than that of residual macrostresses.

Qualitative indications as to the behaviour of residual microstresses in steels on annealing can be obtained directly from measurements of the full width at half maximum of X-ray interference lines. Since broadening of the interference lines is frequently accompanied by an increase in hardness [12], it seems likely that the temperature dependence of the relaxation of residual microstresses in hardened materials is analogous to that of residual macrostresses (see Fig. 2). In this event the relaxation of residual microstresses in hardened materials should occur at lower temperatures, in machined materials at medium and in deformed materials at higher temperatures.

Experimental investigations of the residual macro- and microstress-relaxation of non ferrous materials (titanium alloy TiAl6V4 [20,22], CuZn alloys and AlMg alloys [26]) show that the behaviour is similar to that of steels. An example is represented in Fig. 3. The relative residual macrostresses of pure Al and AlMg alloys, produced by quenching of cylindrical specimens from 450°C in ice water, are plotted as a function of the homologous temperature T/T_m (T_m in this case has the meaning of the liquidus temperature). As it can be seen, quenching residual stresses in Al are relaxed at lower temperatures as in AlMg alloys. Additionally, it seems that a shift of the isochrones to higher temperatures occurs with increasing magnesium content or decreasing stacking fault energy.

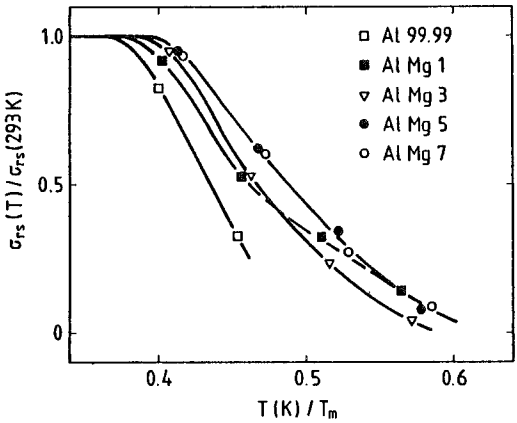

Fig. 3 $\sigma_{rs}(T)/\sigma_{rs}(293K)$ versus T/T_m of pure aluminium and AlMg alloys, quenched (450°C → 0°C) and annealed 1 h [26].

Materials with surface residual stresses, produced by machining or shot peening, frequently show different behaviour in the residual stress-relaxation behaviour of the surface layer with some micrometer thickness and of areas beneath the surface. In most cases, this behaviour is connected with work hardening gradients. Characteristic examples of a shot peened plain carbon steel with 0.45 wt.-% carbon (German grade Ck 45) in different heat treated conditions are shown in Fig. 4 [26]. Residual stress distributions after shot peening and after annealing are given as a function of the distance from the surface after removing small surface layers electro-chemically. As Fig. 4a illustrates, shot peening residual stresses in the hardened state are reduced by annealing of 1 h at 300°C always nearly 50% in the surface and in the depth of the maximum of compressive residual stresses. However, in quenched and tempered condition and also in normalized condition (cf. Fig. 4b and 4c) enlarged relaxation effects are observed in the surface layer and relaxation rate decreases with increasing distance from surface. After deliberate annealing treatments this behaviour holds to completely relaxed residual stresses in the near surface layers in contrast to the interior, where remaining residual stresses exist (see Fig. 4c after annealing 30 min at 550°C). These findings have to be taken into account at the valuation of residual stress-relaxation of corresponding components.

In order to analyse the thermally activated processes responsible for residual stress-relaxation, the influence of time as well as that of temperature must be known. If the time and temperature ranges are sufficiently restricted and if $\sigma_{rs}(T)/\sigma_{rs}(293K)$ = constant (abbreviated in the following to $\sigma_{rs}/\sigma_{rs,0}$) the relationship

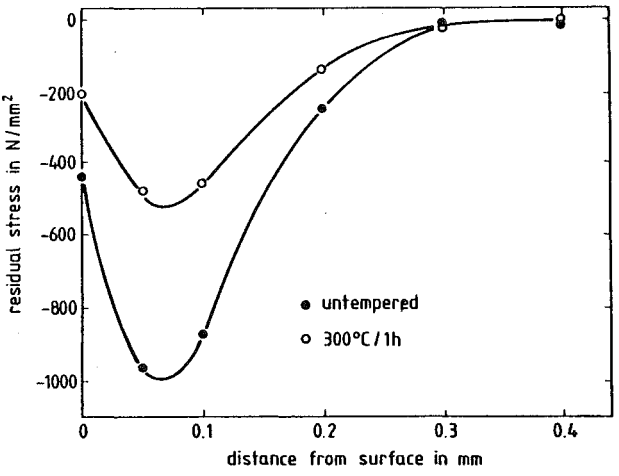

Fig. 4a

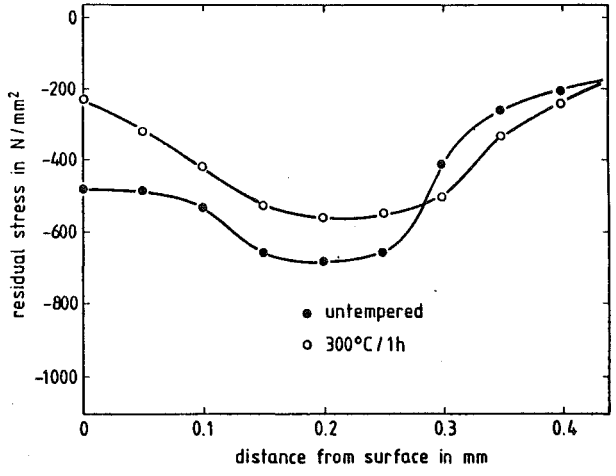

Fig. 4b

$$t = t_o \exp(Q/kT) \tag{2}$$

should hold between annealing time t and annealing temperature T. t_o is a time constant, k is the Boltzmann constant and Q is the activation energy for the t-T range under consideration. Data in the form of σ_{rs}-lgt diagrams in [19] for deformed and hardened steels are not suited to a direct evaluation using Eq. 2.

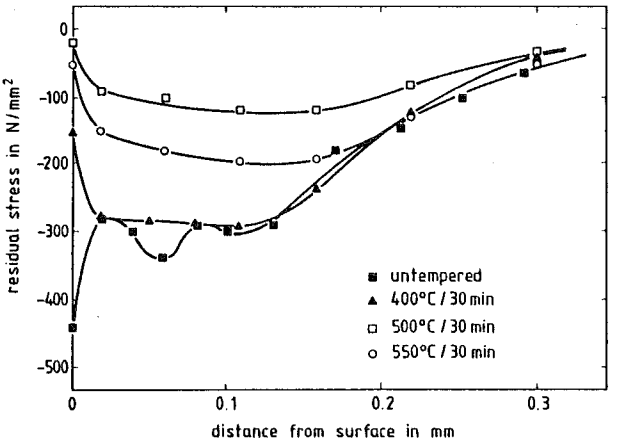

(c)

Fig. 4c

Fig. 4 Shot peening residual stresses of Ck 45 versus distance from the surface before and after annealing [26]: (a) hardened, (b) quenched and tempered (400°C/2h), (c) normalized.

The effect of time on residual stress-relaxation can be linearized with the help of a Zener-Wert-Avrami function [27] to

$$\sigma_{rs}/\sigma_{rs,0} = \exp\,[-\,(At)^m] \tag{3}$$

where m is numerical term dependent on the dominant relaxation mechanism [27,28] and where A is a function dependent on material and temperature

$$A = B \exp\,(-Q/kT). \tag{4}$$

B is a constant. It follows from Eq. 3 that

$$\lg\ln(\sigma_{rs,0}/\sigma_{rs}) = m\lg t + m\lg A \tag{5}$$

with the result that for constant annealing temperatures a plot of $\lg\ln(\sigma_{rs,o}/\sigma_{rs})$ against lgt gives a straight line. Experimental confirmation of this is shown in Fig. 5 for a shot peened titanium alloy (TiAl6V4) [20]. The slopes of the lines are practically independent of the annealing temperature and have a mean value of m = 0.28.

Corresponding annealing temperatures and times for $\sigma_{rs}/\sigma_{rs,o}$ = constant can be derived from such plots. Examples of relaxation of macrostresses and microstresses are given in the lgt-1/kT plot in Fig. 6. The values measured for $\sigma_{rs}/\sigma_{rs,o} = 0.5$ in TiAl6V4 lie on almost perfectly straight lines. Based on Eqs. (4) and (5)

$$\lg t = \text{const.} + \frac{Q}{\ln 10 \cdot kT} \tag{6}$$

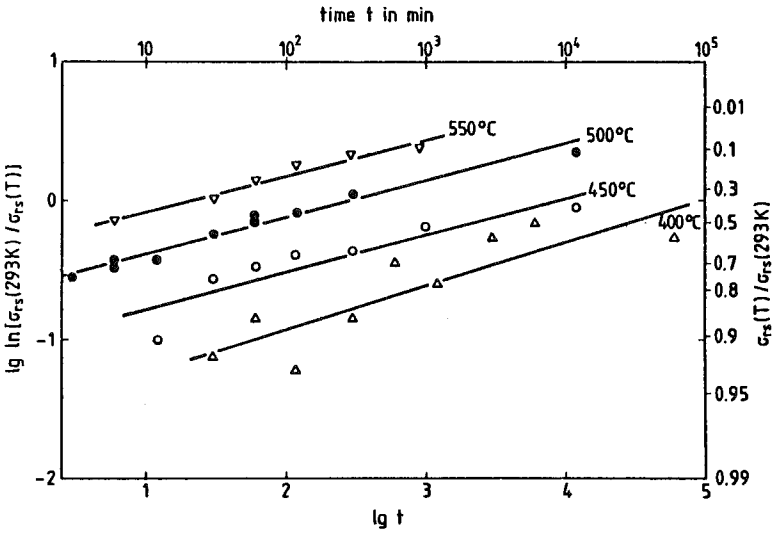

Fig. 5 Influence of annealing time on residual stresses of shot peened TiAl6V4 in a lgln [σ_{rs}(293K)/σ_{rs}(T)]-lgt diagram [20].

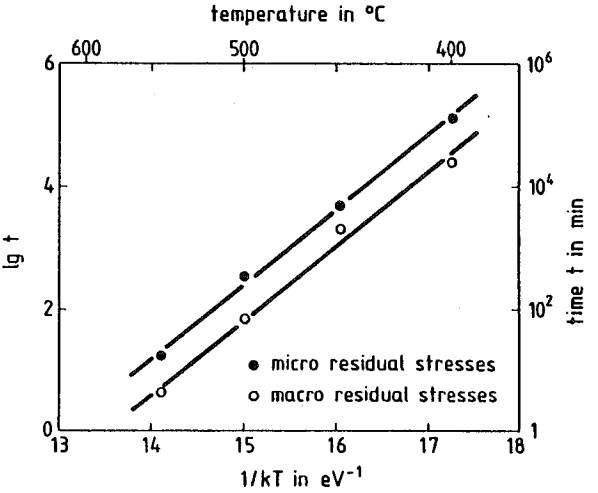

Fig. 6 lgt-1/kT diagram of shot peened TiAl6V4 at residual stress-relaxation of 50% (σ_{rs}(T)/σ_{rs}(293K) = 0.5) [20].

which can be rearranged to give Eq. (2). This yields the activation energy Q = 2.78 eV for macro- and micro-residual stress-relaxation of TiAl6V4. In the

case of this titanium alloy clearly only one process for relaxation of shot peening residual stresses is operative.

A complete quantitative description of the relaxation of macroresidual stresses is of practical importance. For shot peened TiAl6V4 this intension is made possible by Eq. (3) with experimentally determined mean values Q = 2.78 eV, m = 0.28 and the calculated constant $B = 5.4 \cdot 10^{13} s^{-1}$ [20]. In Fig. 7 calculated isochrones of the residual stress-relaxation for t = 10, 60, 10^3 and 10^5 min are represented. There is an optimal agreement between measured values (t = 60 min) and the calculation. For the shot peened states investigated the relaxation starts at about 280°C (553 K) for annealing times of t = 60 min. At about 650°C (923 K) the relaxation is finished. Furthermore, for annealing times > 10^3 min a considerable residual stress relaxation must be taken into consideration for temperatures lower than 300°C (573 K).

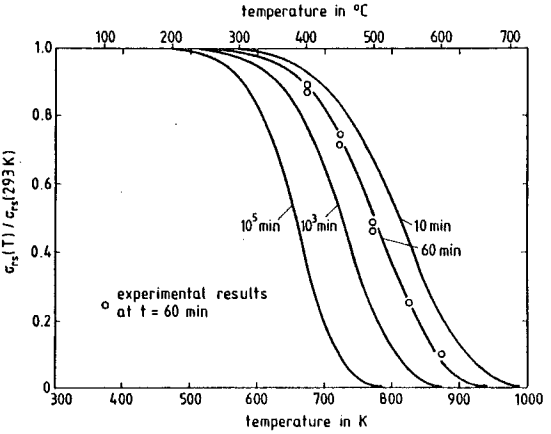

Fig. 7 Temperature dependence of residual stress ratio $\sigma_{rs}(T)/\sigma_{rs}(293K)$ of shot peened TiAl6V4, calculated with mean values of m, B and Q, in comparison with measured residual stress values [20].

A similar discussion of thermally activated processes was carried out for steels [11,12,26], AlMg alloys and CuZn alloys [26] with surface residual stresses of a variety of origins. In the case of steels the activation energy Q depends on the state of the material and lies in the range 1.1 to 2.6 eV. Q is lowest for relaxation of residual stresses due to hardening and highest for those due to deformation in soft annealed states. That proves unequivocally that residual stress-relaxation in steels occurs by several processes.

The activation energies Q obtained for relaxation of shot peening residual stresses in different materials [20,26] are shown in Fig. 8 related to the activation energies Q_o for self diffusion or high temperature creep as a function of the homologous temperature $T_{1/2}T_m$ ($T_{1/2}$ = temperature necessary for 50% residual stress-relaxation after a 1 h anneal). With Q_o = 2.6 eV for a α-Fe [29], 2.51 eV for α-Ti [30], 1.84 eV for CuZn30 [31] and 1.47 eV for Al [29], Q/Q_o lies in the range 0.5 to 1.1. Here and in other materials states the tendency exists that the obtained Q/Q_o-values increase with homologous temperature $T_{1/2}/T_m$ [26]. A similar range of Q/Q_o-values is observed in recovery experiments [32,33]. These are attributed to a number of frequently inseparable softening

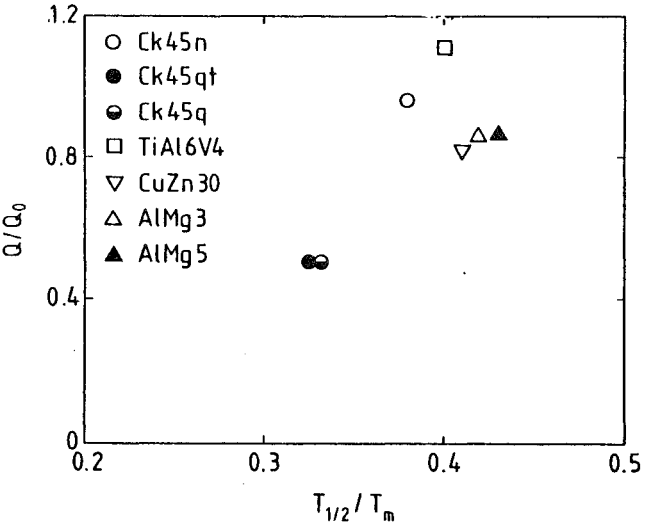

Fig. 8 Activation energy ratios of relaxation of shot peening residual stresses as a function of homologous annealing temperature at t = 1h and $\sigma_{rs}(T)/\sigma_{rs}(293K) = 0.5$ (Q_o = activation energy of self diffusion; n = normalized, qt = quenched and tempered, q = quenched (hardened)).

processes. These processes clearly also dominate residual stress-relaxation and must therefore be dependent on the material and the residual stress state.

Characteristic structural changes occur during the deformation, machining or hardening of steels. Typically, an increase in the dislocation density and a change in the dislocation arrangement are observed. In the case of hardening the concentration of dissolved interstitial atoms differs from the equilibrium value, and this, together with the presence of dislocations, has a decisive influence on the residual stress fields. If a single heat treatment is carried out in the temperature range corresponding to recovery ($T < 0.5\ T_m$) the dislocations adopt arrangements of lower energy by elementary processes such as glide and cross slip by screw dislocations and glide and climb by edge dislocations. In the case of hardened material, diffusion of carbon atoms dependent on the annealing temperature or stage and accompanied by the formation of characteristic carbides is superimposed on these processes.

The rate determining process, with the exception of the early stages in the annealing of hardened steels [13], is clearly the thermally activated climb of edge dislocations [34]. If diffusion of matrix atoms occurs along the edge dislocations to the dislocation core, the activation energy should be $Q = 0.5\ Q_o$. If bulk diffusion predominates the Q value for climb is determined by the activation energy of self diffusion. In the real case both processes occur simultaneously but to different degrees. The dislocation density and arrangement are of considerable importance. In the case of randomly distributed dislocations or tangles of extremely high density, ρ_t, for example in hardened steels ($\rho_t \approx 10^{12}$ to 10^{13} cm^{-2}) residual stress-relaxation is expected to involve dislocation-core diffusion-controlled climb by edge dislocations. Predominantly bulk diffusion

will determine recovery if the dislocation configurations are relatively stable and consist of plane arrangements, cell walls, sub grain or low angle grain boundaries. This recovery process probably occurred in the investigated shot peened non ferrous alloys. In view of the activation energies, the residual stress-relaxation in the deformed steels can probably be classified between these two extremes and occurred by two recovery mechanisms in competition with one another.

According to [13] residual stress-relaxation in hardened rolling bearing steel during the early stages of annealing is due to the diffusion of carbon to dislocations and the formation of Cottrell clouds. This process, which is associated with a reduction in the tetragonality of the martensite lattice should possess an activation energy $\leq Q_i$ (Q_i = activation energy for the diffusion of interstitial atoms; for C in Fe, $Q_i \simeq 0.9$ eV).

With the exception of the early stages in the annealing of hardened steels, residual stress-relaxation in the temperature range corresponding to recovery is a consequence of the rearrangement of dislocations by glide, cross slip and climb. The estimated values of the exponent of the Avrami function $m = 0.1 - 0.3$ [12,26] for steels and non ferrous alloys should be considered in this context. m-values of the same magnitude are observed for the annealing of hardened steels [28] and the formation of GP I zones in AlCu alloys [27]. In [28] this m-value is attributed to the elastic interaction between diffusing carbon atoms and plane dislocation networks or walls. In the case of the examples under discussion it can be assumed from the virtually identical m-values that in the temperature-time range under consideration a similar mechanism is responsible for dislocation rearrangement and hence for residual stress-relaxation regardless of the condition of the materials.

Up to now discussion has centred on residual stress-relaxation at temperatures $T < 0.5\ T_m$, i.e. that brought about by typical recovery processes. In this case mechanical parameters such as hardness and yield point are not significantly altered. During a recrystallization anneal at $T \geq 0.5\ T_m$ the dislocation density rapidly assumes very small values as a result of the growth of new grains. This leads to complete removal of residual macrostresses and to very small residual microstresses but is associated with pronounced changes in the mechanical properties. If extensive reduction is required in the residual stresses in a component without any significant change in yield point or strength, the annealing temperature and time must be chosen to correspond with the recovery stage and not with recrystallization.

Resistance to Stress-Relaxation

Residual stress-relaxtation by heat treatment is fundamentally impossible if in a predominantly uniaxial residual stress state σ_{rs} is smaller than the creep resistance. This resistance, designated in the following by $R_{e,c}$, is characterized by $\varepsilon_p^{\lim} \circ R_{p\varepsilon,c}$, that is by the creep limit at vanishingly small plastic deformation. As shown schematically in Fig. 9, $R_{e,c}$ decreases with increasing temperature and load time. In contrast to industrial creep conditions only very short times are necessary for residual stress-relaxation by creep processes (dislocation creep, grain boundary glide or diffusion creep). With increasing T and/or t, $R_{e,c}$ approaches a localized residual stress peak of magnitude σ_{rs}. For $T = T_{ti}$, σ_{rs} equals $R_{e,c}$ associated with the localized onset of creep deformation. Further increases in temperature or time result in an increasing and measurable microplastic creep strain. As illustrated in Fig. 9, residual stress-relaxation begins at higher temperatures T_{ti} the smaller the load time t_i or the residual stress σ_{rs} and the greater the creep resistance $R_{e,c}$ of the material. Changes in $R_{e,c}$ can be achieved by deliberate alterations in the state of the material. All thermally stable obstacles which have an additional work hardening effect [35] shift the onset of residual stress-relaxation and the entire σ_{rs}-T curve to higher temperatures.

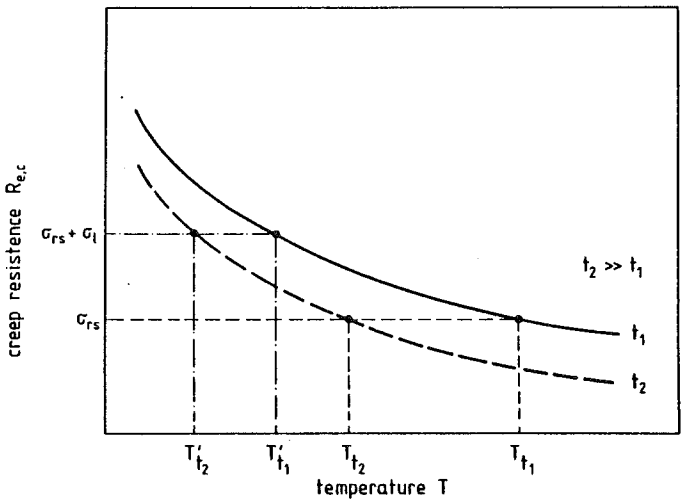

Fig. 9 Creep resistance $R_{e,c}$ versus temperature at different creep times (schematic).

Residual stress-relaxation is also affected by the superposition on a localized residual stress σ_{rs} of an externally applied stress σ_l in the same direction. Increasing σ_l values shift the onset of residual stress-relaxation to shorter times and/or lower temperatures. Applied stresses acting in opposition to the residual stresses in various regions of the material delay the onst of microplastic deformation in these regions. Since the distribution of residual stresses in a component is always inhomogeneous there will be other regions in which superposition of σ_{rs} and σ_l in the same sense promotes plastic deformation. Thus an overall facilitation of residual stress-relaxation can be expected even for applied stresses in the opposing sense.

At this stage it is interesting to explain the result shown in Figs. 1 and 2 where residual stress-relaxation in a deformed sample of Ck 45 is delayed in comparison to that in Ck 22 despite the compressive residual stresses having double the magnitude. Due to its higher carbon concentration Ck 45 contains a greater number of ferrite-cementite phase boundaries than Ck 22. These phase boundaries represent stable obstacles to dislocation glide. They apparently restrict the possibilities for movement of dislocations to arrangements of lower energy required by the recovery process to a greater degree than it is promoted by the increased driving force of the greater residual stress. The delayed residual stress-relaxation in deformed Ck 45 is thus explained by an increase in the creep resistance $R_{e,c}$.

In the case of a multiaxial residual stress state, the residual stress σ_{rs} employed in the arguments given above, must be replaced by an effective residual stress $\sigma_{e,rs}$. If the principal components are $\sigma_{1,rs}$, $\sigma_{2,rs}$ and $\sigma_{3,rs}$, it can be formulated to

$$\sigma_{e,rs} = \frac{1}{\sqrt{2}} \sqrt{(\sigma_{1,rs}-\sigma_{2,rs})^2 + (\sigma_{2,rs}-\sigma_{3,rs})^2 + (\sigma_{3,rs}-\sigma_{1,rs})^2} \qquad (7)$$

on the basis of the shape change hypothesis. The effective residual stress is thus dependent on the differences between the principal residual stress components. These in their turn are proportional to the shear stresses acting on dislocations in the slip systems. Residual stress-relaxation does not therefore occurr for $\sigma_{e,rs} < R_{e,c}$ but does for $\sigma_{e,rs} \geq R_{e,c}$. The case $\sigma_{e,rs} > R_{e,c}$, obtains only briefly since the immediate onset of creep deformation attempts to restore the condition $\sigma_{e,rs} = R_{e,c}$.

The Effect of the Magnitude of the Residual Stresses on Stress-Relaxation

The data in Figs. 1 and 2 show clearly that the residual stress-relaxation in machined or hardened steels occurs more quickly or at lower temperatures, the greater the magnitude of the residual stresses themselves. This is a consequence of temperature, time and stress dependent processes similar to those observed in so-called primary microcreep. Empirical relationships of the form

$$\varepsilon_p = B(T)\sigma^p t^q \tag{8}$$

can be established for constant applied stress σ [6,36]. B is a quantity depending on the temperature and the condition of the material. For the powers, $p \gg 1$ and $0 < q < 1$. The creep strain increases with applied stress and with time. Residual stres-relaxation cannot, however, be compared directly to a creep test. It is much more like a stress relaxation experiment. In the latter case the total strain remains constant while elastic strain is transformed into plastic strain. The following expressions hold true:

$$\sigma_{rs}/E + \varepsilon_p = \text{const} = \sigma_{rs,o}/E \tag{9a}$$

and

$$\varepsilon_p = (\sigma_{rs,o} - \sigma_{rs})/E. \tag{9b}$$

If $\sigma_{rs,o}$ is based on real values of the residual stress, plastic strain of at maximum several tenths of a per cent are possible after completed residual stress-relaxation ($\sigma_{rs} = 0$), i.e. the deformation is in the microcreep range.

Equations (8) and (9) form the basis for quantitative estimates of the residual stress-relaxation [36]. Multiaxial and inhomogeneous residual stress states are neglected or excluded. Although Eq. (8) cannot be substituted directly in Eq. (9) on account of the variable value of the stress ($\sigma = \sigma_{rs}$) it can be seen qualitatively from a combination of the two expressions that increasing σ_{rs} values lead to a more effective residual stress-relaxation. As a result of the greater driving force, shorter times and/or lower temperatures are necessary. This is in agreement with the experimental results presented.

RESIDUAL STRESS-RELAXATION BY PLASTIC DEFORMATION

Unidirectional Deformation

(a) Characteristic examples. In certain cases in practice, unidirectional deformation is often employed in addition to stress free annealing to relieve residual stresses. For example in the case of shaping, the residual stresses can be reduced by a second shaping stage using a smaller reduction in cross sectional area. This can be achieved by redrawing, rerolling, repressing, straightening, mechanical polishing and shot peening [37,38]. Apart from the last, however, these techniques can be used only on simply shaped components

with a uniform cross section. In the case of welded seams a unidirectional load is applied to reduce or redistribute internal stresses [5]. When a critical value of the stress is exceeded directed dislocation movement transforms the elastic strain associated with the residual stress into plastic strain.

Several typical examples will serve to illustrate the relaxation of residual stresses due to shaping, machining, heat treatment and joining by unidirectional deformation. Figure 10 shows the effect of drawing [3] on the behaviour of longitudinal compressive residual stresses at the surface of precipitation-hardened AlCuSiMg alloy (type 2014-T6) and AlZnMg alloy (type 7075-T6). Considerable residual stress-relaxation is achieved up to a deformation of 0.5%. A residue remains which is unaffected by further drawing.

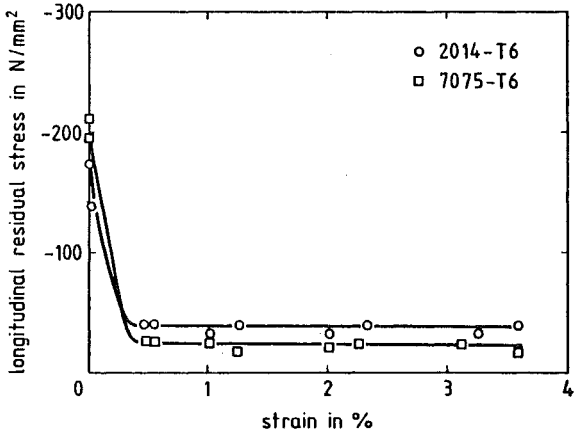

Fig. 10 Relaxation of rolling residual stresses of an AlCuSiMg alloy (2014-T6) and an AlZnMg alloy (7075-T6) due to drawing [3].

Figure 11 shows an example of the relaxation of residual stresses due to surface machining [21,39]. Shot peened specimens of a precipitation hardening AlCu5Mg2 alloy in an optimally hardened condition with coherent precipitates behaves differently under tensile and compressive load. The compressive residual stresses σ^s_{rs} of about - 300 N/mm² in the surface were reduced by about 85% of the yield point of the non-peened material, Re ≃ 375 N/mm², by a tensile load and by about 47% of the yield point by a compressive load. Residual stress-relaxation occurs much more rapidly in tension than in compression. After a total strain $\varepsilon_t \simeq 2\%$ the residual surface stresses are completely removed (see left hand diagram in Fig. 12). If $\varepsilon_t > 2\%$ the sign of σ^s_{rs} changes due to work hardening. In the case of a compressive load the residual stress-relaxation is incomplete. Minimum values are observed in the full width at half maximum of the X-ray interference lines (cf. right hand diagram in Fig. 12) where the residual stress-relaxation rate is greatest. The minimum of full width at half maximum is more pronounced in the case of compressive stress than tensile stress and occurs at smaller ε_t values.

Figure 13 illustrates the behaviour of pure fcc metals and three carbon steels deformed in tension to relieve residual stresses due to quenching [14]. The relative residual stress $\sigma_{rs}/\sigma_{rs,o}$ is plotted against the tensile stress σ relative to the 0.01% proof stress ($\sigma/R_{p0.01}$). The absolute values of the compressive surface residual stresses resulting from quenching without

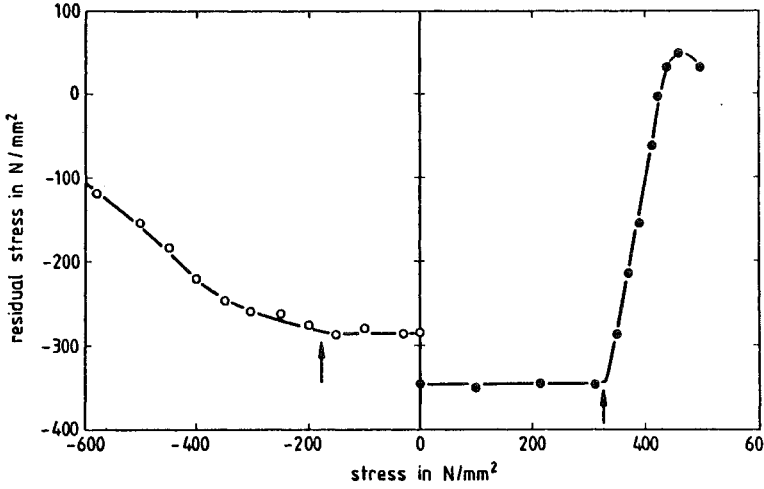

Fig. 11 Relaxation of shot peening residual stresses of an AlCuMg alloy (AlCu5Mg2) due to tensile loading and compressive loading respectively [21,39].

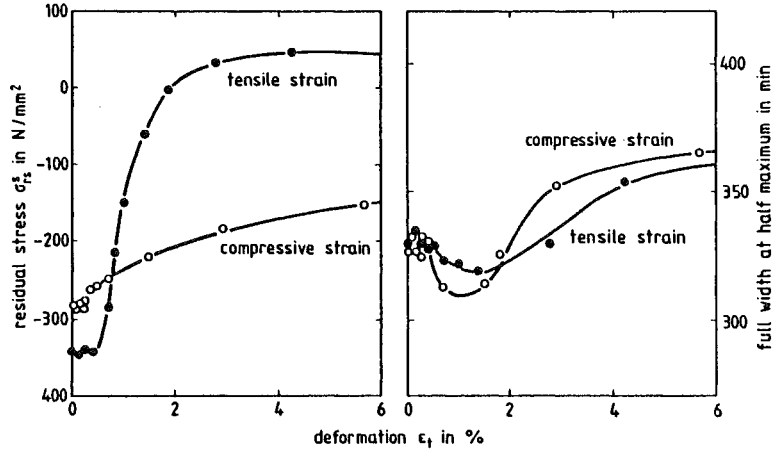

Fig. 12 Residual stresses and full width at half maximum of shot peened AlCuMg2 as a function of total deformation ε_t due to tensile loading and compressive loading respectively [21,39].

transformation $\sigma_{rs,o}$ and the $R_{p0.01}$ values of the unquenched material are also recorded. With a tensile load of up to the 0.01% proof stress the pure fcc metals are residual stress-relaxed relatively rapidly and completely. In the steels, however, residual stress-relaxation is only partial and becomes less

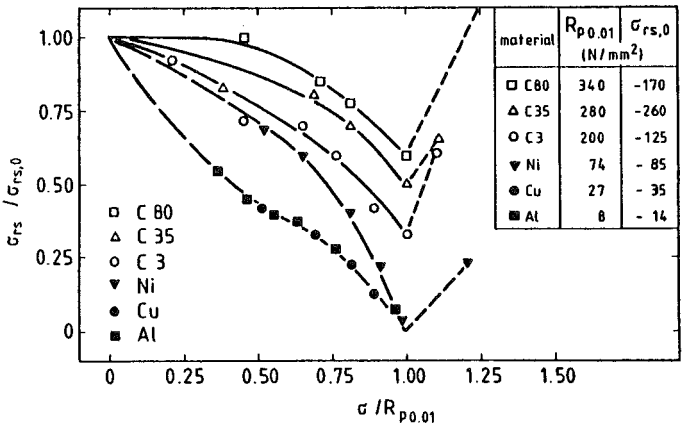

Fig. 13 Quenching residual stress ratio of steels and fcc pure metals as a function of ratio $\sigma/R_{p0.01}$ (σ = tensile stress, $R_{p0.01}$ = 0.01% proof stress) (after [14]).

the greater the carbon content and the higher the yield point. Similar observations are reported in [40]. Loads greater than $R_{p0.01}$ lead to residual deformation stresses which are manifested as increases in the compressive residual stress in the surface. They can be attributed to a macroscopic inhomogeneity in the work hardening between specimen surface and core [14].

In an evaluation of the effect on the strength of residual stresses set up during welding, it is important to know the stability of these stresses on loading the weld. Figure 14 illustrates the considerable reduction in internal stress accompanying tensile loading of an electron beam and TIG welded joint in the martensitic precipitation hardening steel X2 NiCoMo 18 8 5 [41]. In the electron beam welded specimen it begins at about 0.7 R_e, where R_e is the yield point of the unannealed weld. Residual stress-relaxation is not complete. In the case of the TIG weld noticeable residual stress-relaxation first occurs above R_e. By the time the tensile strength R_m is reached, residual stress-relaxation is virtually complete.

Residual stress-relaxation by unidirectional deformation begins at relatively small loads or plastic strains. It may be complete or partial, both the degree and rate of residual stress-relaxation depending on the type and state of the material as well as on the nature of the applied load.

(b) Simple models. First of all the stress-strain behaviour and the residual stress-relaxation of materials with residual stresses can be considered in a rough approximation as illustrated in Fig. 15a in terms of a cylindrical rod with longitudinal residual stresses, namely, constant compressive residual stresses σ^s_{rs} at the surface and constant tensile residual stresses σ^c_{rs} in the core. The surface and core should possess the same yield point and exhibit ideal elastic-plastic deformation behaviour. As shown in the σ-ε_t plot in Fig. 15b the surface stress, σ^s, the core stress σ^c and the mean overall stress $\bar{\sigma}$ increase at first linearly with the total tensile strain ε_t. The core which is subject to residual tensile stresses reaches the yield point R_e at a smaller ε_t value than the surface regions which are subject to residual compressive stresses. Plastic deformation thus commences in the core. If the specimen is

unloaded at $\varepsilon_t < \varepsilon^*_{t(t)}$ the residual stresses remaining overall are reduced. Residual stress-relaxation begins, therefore, when the applied stress $\bar{\sigma}$ reaches the "composite yield point" in tension $\bar{R}_{e(t)}$

$$\bar{\sigma} = \bar{R}_{e(t)} = R_e - \sigma^c_{rs}. \tag{10}$$

On further deformation, the residual stress components of both the surface region and core are reduced linearly with increasing total strain. Above the critical strain $\varepsilon_t = \varepsilon^*_{t(t)}$ the total overall volume deforms plastically at a constant yield stress $\bar{\sigma} = \sigma^s = \sigma^c = R_e$. After unloading no more residual macrostresses are present [8,10]. The critical strain $\varepsilon^*_{t(t)}$ is calculated from the maximum elastic surface deformation by Hooke's law as

$$\varepsilon^*_{t(t)} = (R_e + |\sigma^s_{rs}|)/E. \tag{11}$$

As can be seen from Fig. 15b the $\bar{\sigma}$-ε_t behaviour and the relaxation behaviour of residual stresses under compressive load are anisotropic in comparison to tensile load, because of the different amounts of residual stresses in surface and core ($|\sigma^s_{rs}| > |\sigma^c_{rs}|$). Plastic deformation under compressive load first occurs in the surface region at

$$|\bar{R}_{e(c)}| = R_e - |\sigma^s_{rs}| \tag{12}$$

and residual stress-relaxation is finished at

$$|\varepsilon^*_{t(c)}| = (R_e + \sigma^c_{rs})/E. \tag{13}$$

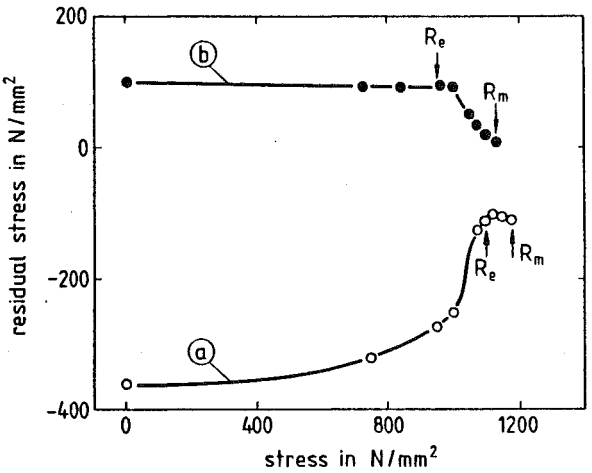

Fig. 14 Relaxation of welding residual stresses of a marageing steel (X2 NiCoMo 18 8 5) due to tensile loading (after [14])
(a) Transversal residual stresses in the welding seam centre of an electron beam welded joint. (b) Transversal residual stresses in a distance of 3 mm of the welding seam centre of a TIG welded joint.

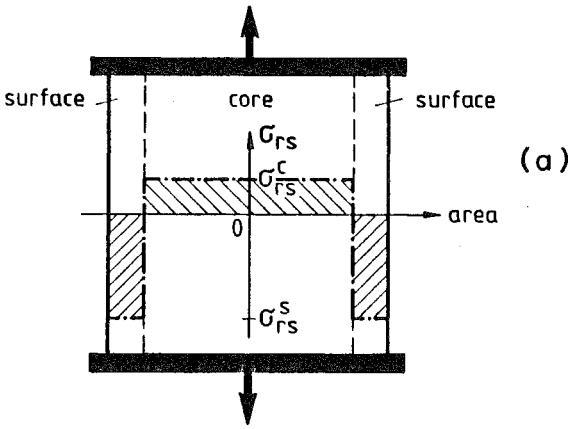

Fig. 15a

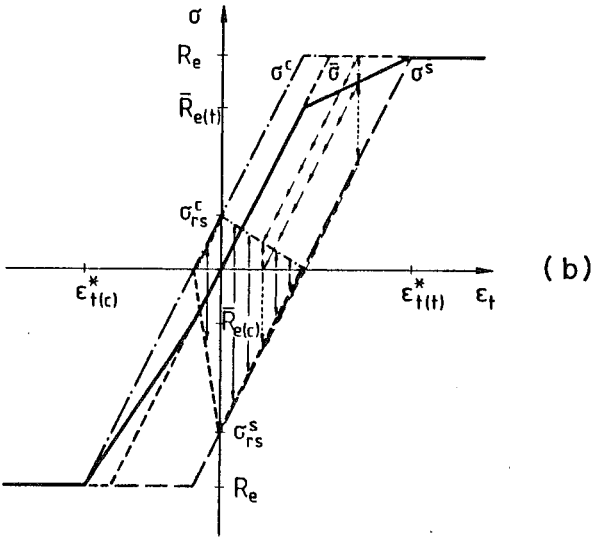

Fig. 15b

If at the same yield point the surface and core harden at the same rate complete residual stress-relaxation is not possible. At sufficiently large total strains in tension and in compression, the residual stresses remaining in surface and core reach a constant value. Residual stress-relaxation is the more pronounced the smaller the work hardening of the material [10].

Stress-strain behaviour and residual stress-relaxation in shot peened specimens under tensile load can quite easily be understood with the help of the right-hand

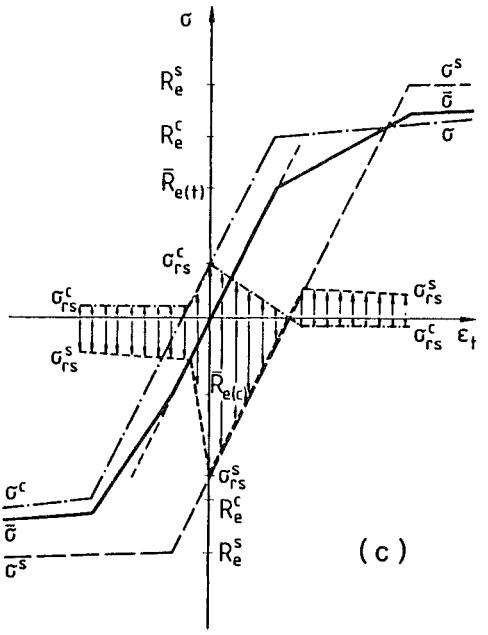

Fig. 15 Simple models for residual stress-relaxation due to uniaxial loading (schematic): (a) Distribution of longitudinal residual stresses, (b) σ-ε_t diagram without work hardening, (c) σ-ε_t diagram with different yield points ($R_e^s > R_e^c$) and linear work hardening.

part of the stress-strain curves in Fig. 15c. It is assumed that the yield point R_e^s in the surface region is greater than that in the core R_e^c as a result of the work hardening effect by shot peening. Furthermore work hardening in uniaxial deformation should occur at a constant rate but less at the surface than in the core. Loading and unloading in the range $\varepsilon_t < \varepsilon^*_{t(t)}$ again lead to residual stress-relaxation, which is more pronounced as the total strain increases. The onset of plastic deformation is determined by the core. A modification of Eq. (10) holds for the composite yield point

$$\bar{R}_{e(t)} = R_e^c - \sigma_{rs}^c. \tag{14}$$

When the total strain $\varepsilon^*_{t(t)}$ is reached and the specimen is unloaded, the original residual stresses are completely removed. Beyond $\varepsilon^*_{t(t)}$, however, further residual stresses are set up as a result of inhomogeneous deformation, namely tensile in the surface regions and compressive in the core.

Residual stress-relaxation under compressive load can be understood by analogy. Stress-strain curves are plotted in the left hand part of Fig. 15c using the same values for σ_{rs}^s, σ_{rs}^c and R_e^s, R_e^c as under tensile load. Plastic deformation first occurs in the surface region at

$$|\bar{R}_{e(c)}| = |R_e^s| - |\sigma_{rs}|. \qquad (15)$$

In contrast to the tensile experiment, residual stress-relaxation in this case is only partial. These findings are in qualitative agreement with the experimental results represented in Figs. 11 and 12.

Now Eq. (15) enables the evaluation of the surface yield point R_e^s using the results for shot peened AlCu5Mg2 given in Figs. 11 and 12. With shot peening induced surface residual stress $\sigma_{rs} = -280$ N/mm² and composite yield point under compressive load $\bar{R}_{e(c)} = -175$ N/mm² Eq. (15) results in $R_e^s = 455$ N/mm² for the yield point of the surface region. This value is about 20% higher than the yield point for unpeened material ($R_e = R_e^c = 375$ N/mm²). That means that shot peening leads to surface hardening. Adequate experiments for shot peened AlCu5Mg2 in different heat treated conditions and for shot peened TiAl6V4 and the evaluation of the surface yield points show that the amount of work hardening is sensitively dependent on the material state [21,22,39].

Table 1 gives the composite yield point $\bar{R}_e$ in terms of the resistance to residual stress-relaxation for applied tensile and compressive load and for sign reversal of the residual stresses. Assuming that cross section areas of surface and core $A^s < A^c$, Eqs. (14) and (15) are valid for both surface hardening ($R_e^s > R_e^c$) and softening ($R_e^s < R_e^c$).

TABLE 1 Composite Yield Point $\bar{R}_e$ in terms of the resistance to residual stress -relaxation ($A^s < A^c$, $|R_e^s| \gtrless |R_e^c|$)

Residual stress state	Composite yield point for applied tensile load	Composite yield point for applied compressive load
Surface compressive residual stresses and core tensile residual stresses	$\bar{R}_{e(t)} = R_e^c - \sigma_{rs}^c$	$\lvert\bar{R}_{e(c)}\rvert = \lvert R_e^s\rvert - \lvert\sigma_{rs}^s\rvert$
surface tensile residual stresses and core compressive residual stresses	$\bar{R}_{e(t)} = R_e^s - \sigma_{rs}^s$	$\lvert\bar{R}_{e(c)}\rvert = \lvert R_e^c\rvert - \lvert\sigma_{rs}^c\rvert$

Actual materials usually possess a continuous residual macrostress profile over the cross section of the specimen. If, for example, residual compressive stresses associated with work hardening are present in the surface region and tensile stresses are present in the core, σ_{rs}^s (cf. Fig. 15c) represents the maximum residual compressive stress in the surface region and σ_{rs}^c represents the maximum tensile stress in the core. Taking this into account, then in the case of a predominantly uniaxial internal stress state, Eqs. (14) and (15) can be used to assess the onset of residual stress-relaxation and Eqs. (11) and (13) its completion. In the latter situation R_e is replaced by R_e^s or R_e^c. In agreement with the experimental findings presented above, residual stress-relaxation begins at a tensile load (compressive load) for $\sigma_{rs}^c > 0$ ($\sigma_{rs}^c < 0$) in the range $0 < |\bar{\sigma}| < |R_e^c|$ or for $\sigma_{rs}^s > 0$ ($\sigma_{rs}^s < 0$) in the range $0 < |\bar{\sigma}| < |R_e^s|$. It is complete under the condition $|\sigma_{rs}^s| < |R_e^s|$ or $|\sigma_{rs}^c| < |R_e^c|$ according to Eqs. (11) and (13) at $|\varepsilon_t^*| < 2\,|R_e^s|/E$ or $|\varepsilon_t^*| < 2\,|R_e^c|/E$.

In the case of a multiaxial residual stress state with an applied stress σ_1 acting in the direction of greatest principal residual stress $\sigma_{1,rs}$, residual stress-relaxation begins when the local value of the effective stress $\sigma_e = f(\sigma_1 + \sigma_{1,rs}; \sigma_{2,rs}; \sigma_{3,rs})$ reaches the yield point R_e^i. Based on the shape change energy hypothesis

$$R_e^i = \sigma_e = \frac{1}{\sqrt{2}} \sqrt{(\sigma_1+\sigma_{1,rs}-\sigma_{2,rs})^2 + (\sigma_{2,rs}-\sigma_{3,rs})^2 + (\sigma_{3,rs}-\sigma_1-\sigma_{1,rs})^2}. \quad (16)$$

If the yield point is the same for the surface region and core ($R_e^i = R_e^s = R_e^c$) and the principal component of the residual stress $\sigma_{1,rs} = \sigma_{rs}$, a greater applied stress σ_1 is needed to induce residual stress-relaxation than in the uniaxial case (cf. Eq. (14)) due to inhibition of slip.

A quantitative description of the relaxation of multiaxial residual macrostresses with a known profile over the component cross section has proved to be extremely difficult. Even using simple, one dimensional models the computations are substantial [42,43].

(c) The behaviour of residual microstresses. Residual microstresses behave in a complex fashion during the relaxation of residual macrostresses by unidirectional deformation. So far only isolated experimental data based on X-ray profile analysis are available relating to this area.

When a material is shaped or machined, both directed and inhomogeneous residual microstresses are set up. Those of the first type are the result of backstresses due to dislocation pile ups at boundary surfaces and elastic strained second phases of heterogeneous materials. If these dislocations move in the reverse direction during localized plastic deformation, the back-stresses and hence the directed residual microstresses are initially reduced. Further deformation causes renewed build up of backstresses in the opposing direction associated with dislocation multiplication and hardening which must once again increase the residual microstresses.

Dislocation arrangements in a random distribution or in tangles or cells give rise to inhomogeneous residual microstresses. Microplastic deformation can lead to the rearrangement of dislocations into arrangements of lower energy and thus bring about residual microstress-relaxation. If new dislocations are produced, a renewed build up of residual microstresses is superposed on the relaxation process. This provides an explanation of the behaviour of the full width at half minimum for an aluminium alloy under unidirectional deformation described above (cf. Fig. 12).

A reduction in the residual microstresses in hardened steels is observed both on deformation [44] and on machining [23,45,46]. Two superimposed effects can operate here. After hardening, a very high density of dislocations is present either randomly distributed or in tangles [25,48]. Microplastic deformation brings about a rearrangement of these dislocations into configurations with lower distortion energy and therefore a reduction in the residual microstresses. On the other hand dissolved carbon atoms may be induced to diffuse into the energetically more favourable octahedral interstices in the martensite lattice under the influence of the stress field of the moving dislocations. This causes a reduction in the tetragonality and hence the lattice distortion due to dissolved carbon atoms.

Deformation under Cyclic Stress

The fatigue strength of metallic materials can be influenced quite considerably by residual stresses. Since in certain cases they can be considered as locally

variable intermediate stresses, they can lead to substantial increases in the fatigue strength (cf. for example, [2,4,7,8,10,11,48]). The influence of residual stresses on the processes in the precrack free stage of cyclic deformation is of particular importance. Coupled with this is the stability of the residual stresses.

It has been shown in numerous investigations (cf. for example, [4,7,11,17,18,23, 45,46,49]) that the effect of residual stresses decreases with increasing stress amplitude and number of cycles as a result of residual stress-relaxation. This is exemplified in Fig. 16 by a shot peened aluminium alloy (AlCu5Mg2) which has undergone a reverse bending fatigue test [21,39]. The residual macrostresses on the front and reverse sides of flat specimens are plotted against the number of cycles to fracture for three different stress amplitudes σ_a. The greatest residual stress-relaxation occurs during the first cycle in every case. It is particularly pronounced at the greatest stress amplitude σ_a = 325 N/mm². It should be noted that in the first half of the cycle there is a considerable reduction in the residual compressive stresses on the front face of the specimen, which is in compression, whereas in the second half of the cycle, when the reverse side of the specimen is in compression, residual compressive stresses in this face are reduced to a value of about 200 N/mm². After the first cycle there is little further reduction in residual stress.

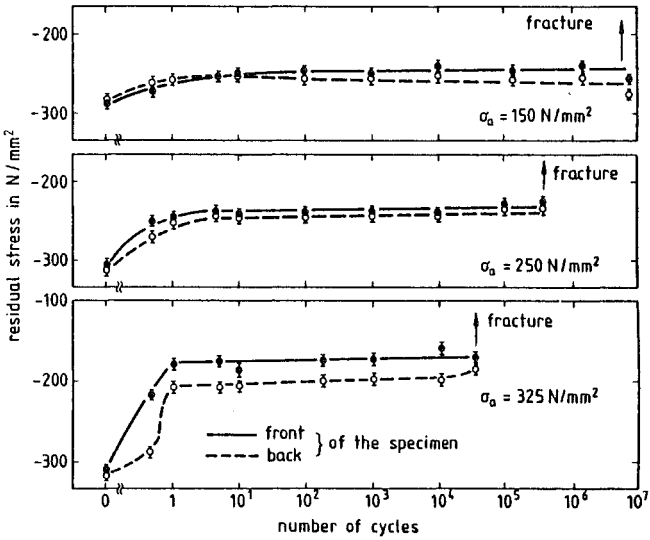

Fig. 16 Relaxation of shot peening residual stresses of an AlCuMg alloy (AlCu5Mg2) due to cyclic bending with several stress amplitudes σ_a [21,39].

Additional examples of the relaxation of machining residual stresses, effected by cyclic bending deformation are represented in Fig. 17 for the plain carbon steel Ck 45 in different heat treated conditions [46]. In the normalized state surface tensile residual stresses, produced by face-milling decrease with increasing stress amplitude and number of cycles. The relaxation is completed immediately before fracture (marked by arrows in Fig. 17a). In Fig. 17b the relaxation behaviour of grinding residual stresses of different sign is shown for Ck 45 in a quenched and tempered state. In this case specimens with

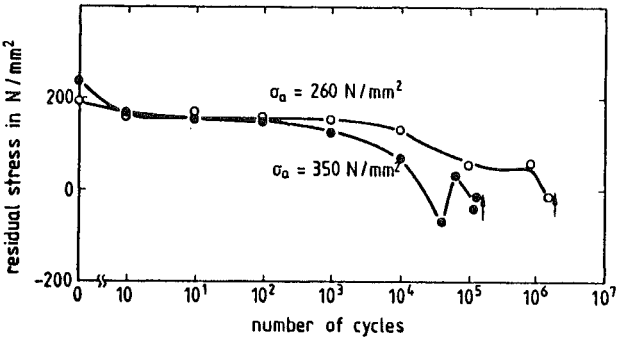

Fig. 17a

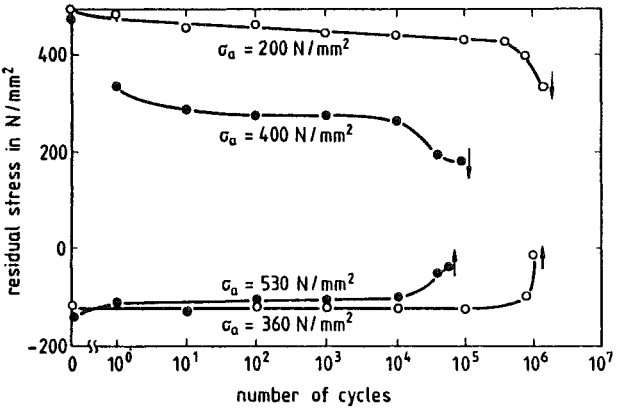

Fig. 17b

compressive residual stresses also relax completely, in contrast to the condition with surface tensile residual stresses. Finally Fig. 17c represents the result of cyclic bending on the surface grinding residual stresses with different sign of hardened Ck 45. As it can be seen, the amount of residual stress relaxation is relatively insignificant.

The remaining surface residual stresses at fracture (number of cycles $N = N_f$) determine significantly the fatigue life of materials. In this context the results of a variety of shot peened materials (AlCu5Mg2 in different states [21], TiAl6V4 [22], Ck 45 quenched and tempered [49], 16MnCr5 blank-hardened [45]) are of great importance. In the left-hand diagram all materials show a pronounced residual stress-relaxation with increasing stress amplitude. The normalized representation in the right-hand diagram in Fig. 18 provides an impressive illustration of this behaviour. σ_a is divided by the yield point in the surface region R_e^s obtained from compression tests. The residual compressive stresses $\sigma_{re}^s(N_f)$ remaining after fracture ($N = N_f$) in completely different materials now lie on the same curve.

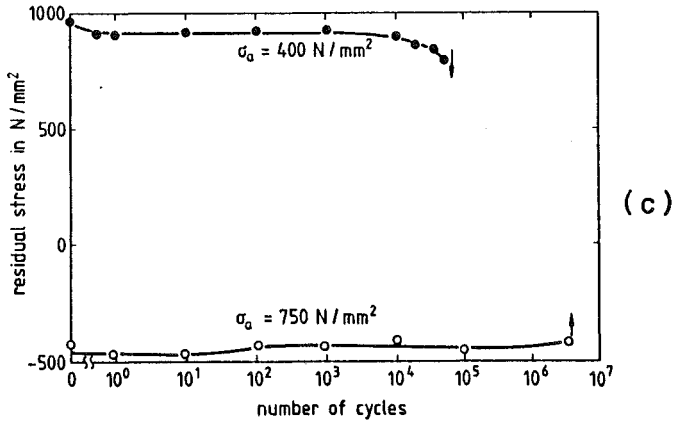

Fig. 17c

Fig. 17 Relaxation of machining residual stresses of a plain carbon steel with 0.45 wt.-% carbon (German grade Ck 45) in different heat treated conditions due to cyclic bending with several stress amplitudes σ_a [46]. (a) normalized state; face-milling residual stresses, (b) quenched and tempered state (600°C/2h); grinding residual stresses, (c) hardened state; grinding residual stresses.

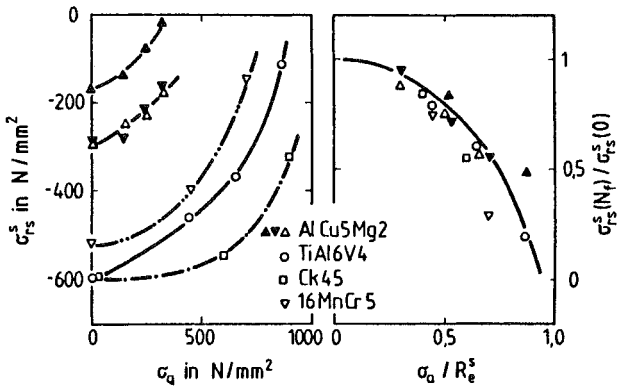

Fig. 18 Surface residual stresses after fatigue fracture as a function of stress amplitude of different shot peened materials [21,22,45,49] (▼ AlCu5Mg2 as received, △ AlCu5Mg2 under-aged, ▲ AlCu5Mg2 peak-aged, o TiAl6V4, ■ Ck 45, ▽ 16MnCr5).

Figure 18 incorporates the three most important parameters affecting residual stress-relaxation. These are the yield point R_e characteristic of the material (or the yield point in the surface region R_e^s), the stress amplitude σ_a appropriate to the type of loading and the initial residual stress $\sigma_{rs}(0)$. Based on these three parameters, it has been possible to achieve a systematic classification of much of the available data [4,7,11]. At this point, therefore, a discussion of some aspects bearing in mind the problems mentioned in the preceding section should suffice.

Assuming a predominantly uniaxial residual stress state, it is a fundamental principle that residual stress-relaxation will commence within the first cycle (N = 1) of an alternating load if the stress amplitude reaches the composite yield point ($\sigma_a = \bar{R}_e$). The quasistatic relaxation processes described in section 3.1 will then take place. It should, however, be noted that, according to Eq. (14) and (15), different composite yield points apply in the first tensile and compressive half-cycle (cf. also Table 1). If $\sigma_a < \bar{R}_e$, the residual stresses should remain stable in the first cycle. For N > 1, residual stress-relaxation can begin gradually if at least the composite cyclic yield point $\bar{R}_{e,cyc}$ is exceeded [10,48]. It is necessary that

$$\sigma_a \geq \bar{R}_{e,cyc}.$$

Equations (14) and (15) are equally valid for the cyclic composite yield point if R_e^s and R_e^c are replaced by the corresponding cyclic yield points for surface and core. Applying the boundary conditions given in Table 1, then

$$\bar{R}_{e,cyc} = R^c_{e,cyc} - \sigma^c_{rs} \tag{17}$$

or

$$\bar{R}_{e,cyc} = R^s_{e,cyc} - \sigma^s_{rs} \tag{18}$$

depending on whether cyclic plastic deformation begins in the core or at the surface. If no cyclic plastic or quasiplastic deformation occurs, then

$$\sigma_a < \bar{R}_{e,cyc} \quad \text{and} \quad \sigma_a < \bar{R}_e$$

which ensures the existence of a stable residual stress state under alternating load [10,48].

A summary of the different cases of relaxation behaviour discussed above is illustrated schematically in Fig. 19 in a σ^s_{rs}-N diagram. At a constant stress amplitude the cases (4), (3), or (2) and (1) occur actual one and another with increasing yield point or surface yield point, in agreement with the findings in Fig. 18.

Residual stress-relaxation when N > 1 (cases (2) and (4) in Fig. 19) can be attributed to cyclic plastic deformation. In this case the dislocation arrangements present in the starting material are rearranged to configurations characteristic of the fatigued condition for the given stress amplitude. Especially for cold worked materials dislocation rearrangements are frequently associated with the softening processes in the precrack free stage of fatigue [50,51].

Rearrangement of dislocations from configurations typical of the machined or heat treated conditin of that of the fatigued state is fundamental to the relaxation of macrostresses. Residual elastic strains associated with the residual stresses are once again transformed into microplastic strains. If fatigue softening processes are involved relaxation of microstresses can also be expected. In the case of machined and heat treated materials this manifests itself in decreasing hardness and sharper X-ray interference lines [23,45,46,49] Differences in the residual stress-relaxation behaviour of cold worked, machined and heat treated materials under cyclic load can be attributed to different dislocation arrangements and densities. The closer the similarity to the

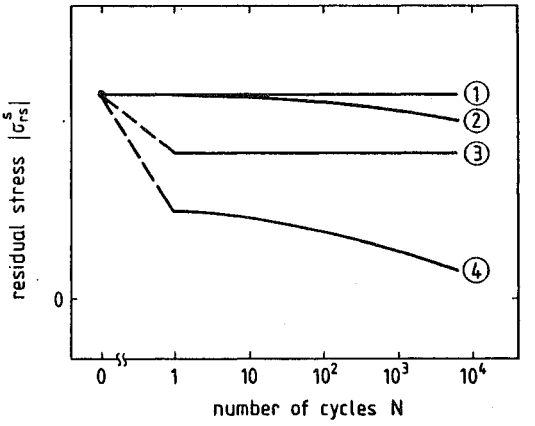

Fig. 19 Behaviour of surface residual stresses at cyclic loading in a $|\sigma_{rs}^s|$-N diagram (schematic) (1) $\sigma_a < \bar{R}_e$ and $\sigma_a < \bar{R}_{e,cyc}$, (2) $\bar{R}_e > \sigma_a > \bar{R}_{e,cyc}$, (3) $\bar{R}_{e,cyc} > \sigma_a > \bar{R}_e$, (4) $\sigma_a > \bar{R}_e$ and $\sigma_a > \bar{R}_{e,cyc}$.

dislocation configuration characteristic of fatigue the less the extent of dislocation rearrangement and hence of residual stress relaxation.

SUMMARY AND CONCLUSIONS

Residual stress-relaxation by heat treatment or under unidirectional or cyclic mechanical stress is brought about essentially by the movement of dislocations. This converts the elastic strains related to residual stresses into microplastic deformation. The onset of residual stress-relaxation is dependent on the resistance R_i to the onset of plastic deformation. In the case of unidirectional deformation $R_i = R_e$, cyclic loading $R_i = R_{e,cyc}$ and heat treatment $R_i = R_{e,c}$. In principle, residual stress-relaxation occurs when the linear superposition of applied and residual stress reaches the material resistance R_i assuming a predominantly uniaxial state according to

$$\sigma + \sigma_{rs} = R_i \tag{19}$$

Residual stress-relaxation does not occur if the condition

$$\sigma + \sigma_{rs} < R_i \tag{20}$$

is fulfilled.

The applied stress σ may be zero, have a value which does not vary with time (cf. thermal residual stress-relaxation), have a steadily increasing value (cf. unidirectional deformation) or a value varying periodically with time (cf. cyclic deformation). Since, according to Eq. (19), the onset of residual stress-relaxation depends on the resistance of the material R_i as well as on the applied stress σ, all the parameters characterizing the state of the material as well as temperature and time or frequency make themselves felt. The onset of stress-

relaxation is delayed by the presence of sufficient stable obstacles to dislocation movement which increases R_i at the loads given. For $T < 0.4\ T_m$ these could, for example, be grain and phase boundaries, finely dispersed incoherent particles, coarse secondary phases and, as long as no diffusion can occur, dissolved impurity atoms and certain dislocation arrangements. The onset and extent of residual stress-relaxation are influenced in a complex fashion by the combined effects of heat treatment, unidirectional and cyclic stress and by multiaxial applied and/or residual stress states. The kinetics of residual stress-relaxation are determined essentially by the difference $\sigma + \sigma_{rs} - R_i$. The rate increases the greater the applied load, i.e. the higher the temperature, the longer the time and the greater the magnitude and amplitude of the applied stress, plastic deformation or number of cycles. It often increases as the amount of residual stress increases. The rate is faster the fewer the stable obstacles to dislocation glide.

REFERENCES

[1] Peiter, A. (1966) Eigenspannungen 1. Art. Ermittlung und Bewertung. Triltsch Verlag, Düsseldorf.

[2] Munz, D. (1967) Der Einfluß von Eigenspannungen auf das Dauerschwingverhalten. Härterei-Tech. Mitt. 2, 52-62.

[3] Barker, R. S. and J. G. Sutton (1967) Stress Relieving and Stress Control. In "Aluminium", Vol. III (ed. by K. R. Horn). ASM, Metals Park/Ohio.

[4] Wohlfahrt, H. (1973) Zum Eigenspannungsabbau bei der Schwingbeanspruchung von Stählen. Härterei-Tech. Mitt. 28, 288-293.

[5] Ruge, J. (1974) Handbuch der Schweißtechnik. Chapter 23.5 "Eigenspannungen". Springer-Verlag, Berlin.

[6] Marschall, C. W. and R. E. Maringer (1977) Dimensional Instability. Pergamon Press, New York.

[7] Wohlfahrt, H. (1978) Einfluß von Eigenspannungen. In: "Verhalten von Stahl bei schwingender Beanspruchung" (ed. by W. Dahl). Verlag Stahleisen, Düsseldorf, pp. 141-164.

[8] Macherauch, E. (1979) Neuere Untersuchungen zur Ausbildung und Auswirkung von Eigenspannungen in metallischen Werkstoffen. Z.f. Werkstofftechnik 10, 97-111.

[9] James, M. R. and J. B. Cohen (1980) The Measurement of Residual Stresses by X-Ray Diffraction Techniques. In "Treatise on Materials Science and Technology", Vol. 19A (ed. by H. Herman). Academic Press, New York, pp. 1-62.

[10] Macherauch, E. (1980) Bewertung von Eigenspannungen. In "Eigenspannungen". Deutsche Gesellschaft für Metallkunde, Oberursel, pp. 41-67.

[11] Vöhringer, O. and H. Wohlfahrt (1983) Abbau von Eigenspannungen. In: "Eigenspannungen und Lastspannungen". Beiheft der Härterei-Tech. Mitt. (ed. by V. Hauk and E. Macherauch). Hanser-Verlag, München, pp. 144-156.

[12] Vöhringer, O. (1983) Abbau von Eigenspannungen. In: "Eigenspannungen. Entstehung - Messung - Bewertung", Vol. 1 (ed. by E. Macherauch and V. Hauk). Deutsche Gesellschaft fur Metallkunde, Oberursel, pp. 49-83.

[13] Hanke, E. (1969) Snoek- und Cottrell-Effekt, zwei dominierende Diffusionsmechanismen beim Anlassen gehärteten Stahles. Fortschritts-Berichte VDI-Z. Reihe 5, Nr. 9.

[14] Sautter, R. (1965) Gitterdehnungen in verformten und abgeschreckten Metallen. Diploma thesis, TH Stuttgart.

[15] Gärttner, W. (1966) Anomalien in der Eigenspannungsausbildung nach Zugverformung unlegierter und chromlegierter Stähle. Diploma thesis, TH Stuttgart.

[16] Schimmöller, H. (1972) Rechnerische Behandlung der Verlagerung von Eigenspannungen in einem Stabmodell durch Überbelastung. Z.f. Werkstofftechnik 3, 301-306.

[17] James, M. R. and W. L. Morris (1981) The Relaxation of Machining Stresses

in Aluminium Alloys During Fatigue. In: "Residual Stress for Designers and Metallurgists". ASM, Metals Park/Ohio, pp. 169-188.

[18] James, M. R. (1982) The Relaxation of Residual Stresses During Fatigue. In: "Residual Stress and Stress Relaxation" (ed. by E. Kula and V. Weiss). Plenum Press Publ. Corp., New York, pp. 297-314.

[19] Wolfstieg, U. and E. Macherauch (1980) Zum thermischen Abbau von Eigenspannungen. In: "Eigenspannungen". Deutsche Gesellschaft für Metallkunde, Oberursel, pp. 345-354.

[20] Hirsch, T., O. Vöhringer and E. Macherauch (1983) Der thermische Abbau von Strahleigenspannungen bei TiAl6V4. Härterei-Tech. Mitt. 38, 229-232.

[21] Hirsch, T., O. Vöhringer and E. Macherauch (1984) Bending Fatigue Behaviour of Differently Heat Treated and Shot Peened AlCu5Mg2. Proc. 2nd Int. Conf. Shot Peening. Am. Shot Peen. Soc., Paramas, New York, pp. 90-101.

[22] Vöhringer, O., T. Hirsch and E. Macherauch (1985) Relaxation of shot peening induced residual stresses of TiAl6V4 by annealing or mechanical treatment. Proc. 5th Int. Conf. Titanium, Vol. 3 (ed. by G. Lütjering, U. Zwicker, W. Bunk). Deutsche Gesellschaft für Metallkunde, Oberursel, pp. 2203-2211..

[23] Ilg, U. (1980) Strukturelle Änderungen in unterschiedlich wärmebehandelten Wälzkörpern aus 100Cr6 und 20MnCr5 bei Wälz- sowie Wälz-Gleitbeanspruchung. Dr.-Ing. thesis, Universität Karlsruhe.

[24] Faber, H., O. Vöhringer and E. Macherauch, E. (1979) Röntgeninterferenzlinienanalyse an gehärteten und angelassenen Kohlenstoffstählen. Härterei-Tech. Mitt. 34, 1-9.

[25] Vöhringer, O. and E. Macherauch (1977) Struktur und mechanische Eigenschaften von Martensit. Härterei-Tech. Mitt. 32, 153-168.

[26] Hoffmann, J. (1985) Entwicklung schneller röntgenographischer Spannungsmeßverfahren und ihre Anwendung bei Untersuchungen zum thermischen Eigenspannungsabbau. Dr.-Ing. thesis, Universität Karlsruhe.

[27] Fine, M. W. (1965) Introduction to Phase Transformations in Condensed Systems, McMillan Comp., New York.

[28] Lement, B. S. and M. Cohen (1965) A Dislocation-Attraction Model for the First Stage of Tempering. Acta Met. 4, 469-476.

[29] Frost, H. J. and M. F. Ashby (1982) Deformation-Mechanism Maps. Pergamon Press, New York.

[30] Doner, M. and H. Conrad (1973) Deformation Mechanism in Commercial Ti-50A (0.5 at.pct.O_{eq}) at Intermediate and High Temperatures (0.3-0.6 T_m). Metallurg. Trans.4, 2809-2817.

[31] Mayer, M. (1978) Die dynamische Reckalterung von CuZn-, CuNi- und CuNiZn-Legierungen. Dr.-Ing. thesis, Universität Karlsruhe.

[32] Leslie, W. C. (1981) The Physical Metallurgy of Steels. McGraw-Hill Book Comp. New York.

[33] Byrne, J. G. (1965) Recovery, Recrystallization and Grain Growth. McMillan Comp. New York.

[34] Langdon, T. G. (1981) Deformation of Polycrystalline Materials of High Temperatures. In: "Proc. 2. Risø Int. Symp. on Metallurgy and Materials Science. Risø National Laboratory, Roskilde, pp. 45-54.

[35] Macherauch, E. and O. Vöhringer (1978) Das Verhalten metallischer Werkstoffe unter mechanischer Beanspruchung. Z.f. Werkstofftechnik 9, 370-391.

[36] Woodford, D. A. (1979) Creep Analysis of Zircaloy-4 and its Application in the Prediction of Residual Stress Relaxation. Journ. of Nucl. Mat. 79, 345-353.

[37] Peiter, A. (1966) Das Entspannen von Ziehgut durch Strecken, Richten und Anlassen. Z. Metallkunde 57, 1-8.

[38] Neubauer, A., A. Eichhorn and H. Hoffmann (1976) Nachformen - eine neue Methode zur Verringerung der Eigenspannungen 1. Art in Stahlleichtbauprofilen. Wiss. Z. d. TH Otto v. Guericke, Magdeburg 20, 563-569.

[39] Hirsch, T. (1983) Zum Einfluß des Kugelstrahlens auf die Biegeschwingfestigkeit von Titan- und Aluminiumbasislegierungen. Dr.-Ing. thesis, Universität Karlsruhe.

[40] Bühler, H. (1955) Zur Frage der Eigenspannungen in statisch beanspruchten Stäben. Archiv Eisenhüttenwes. 26, 51-54.

[41] Hickel, H., H. Wohlfahrt and E. Macherauch (1973) Zum Dauerschwingverhalten elektronenstrahl- und WIG-geschweißter Bleche des martensitaushärtbaren Stahles X2 NiCoMo18 8. DVS-Bericht 26, Strahltech. VI, pp. 53-56.

[42] Tesar, S. (1970) Verlagerung von Eigenspannungen durch Außenlast. Schweißen und Schneiden 22, 145-150.

[43] Schimmöller, H. (1972) Rechnerische Behandlung der Verlagerung von Eigenspannungen in einem Stabmodell durch Überbelastung. Z.f. Werkstofftechnik 3, 301-306.

[44] Alshevskiy, Y. L. and G. V. Kurdjumov (1970) Influence of Plastic Deformation on the Crystalline Structure of Martensite. Fiz. metal. metalloved. 30, 413-417.

[45] Schreiber, R. (1976) Untersuchungen zum Dauerschwingverhalten des kugelgestrahlten Einsatzstahles 16MnCr5 in verschiedenen Wärmebehandlungszuständen. Dr.-Ing. thesis, Universität Karlsruhe.

[46] Hoffmann, J. E. (1984) Der Einfluß fertigungsbedingter Eigenspannungen auf das Biegewechselverhalten von glatten und gekerbten Proben aus Ck 45 in verschiedenen Werkstoffzuständen. Dr.-Ing. thesis, Universität Karslruhe.

[47] Krauss, G. (1980) Principles of Heat Treatment of Steel. ASM, Metals Park/Ohio.

[48] Macherauch, E. and K. H. Kloos (1983) Bewertung von Eigenspannungen. In: "Eigenspannungen und Lastspannungen". Beiheft der Härterei-Tech. Mitt (ed. by V. Hauk and E. Macherauch). Hanser-Verlag, München, pp. 175-194.

[49] Starker, P. (1981) Der Größeneinfluß auf das Biegewechselverhalten von Ck 45 in verschiedenen Bearbeitungs- und Wärmebehandlungszuständen. Dr.-Ing. thesis, Universität Karlsruhe.

[50] Macherauch, E. and P. Mayr (1977) Strukturmechanische Grundlagen der Werkstoffermüdung. Z.f. Werkstofftechnik 8, 213-224.

[51] Hertzberg, R. W. (1976) Deformation and Fracture Mechanics of Engineering Materials. J. Wiley, New York.